AWARD NUMBER: W81XWH-16-1-0580

TITLE: Flexible Regenerative Nanoelectronics for Advanced Peripheral Neural Interfaces

PRINCIPAL INVESTIGATOR: Aaron B. Baker

CONTRACTING ORGANIZATION: University of Texas at Austin, Austin, TX 78712

REPORT DATE: October 2017

TYPE OF REPORT: Annual

PREPARED FOR: U.S. Army Medical Research and Materiel Command
Fort Detrick, Maryland 21702-5012

# REPORT DOCUMENTATION PAGE

*Form Approved*
*OMB No. 0704-0188*



| 1. REPORT DATE | 2. REPORT TYPE | 3. DATES COVERED |
|---|---|---|
| October 2017 | Annual | 09/30/2016–09/29/2017 |

**4. TITLE AND SUBTITLE**
Flexible Regenerative Nanoelectronics for Advanced Peripheral Neural Interfaces

**5a. CONTRACT NUMBER**

**5b. GRANT NUMBER**
W81XWH-16-1-0580

**5c. PROGRAM ELEMENT NUMBER**

**6. AUTHOR(S)**

Aaron Baker and Chong Xie

E-Mail: abbaker@austin.utexas.edu and chongxie@utexas.edu

**5d. PROJECT NUMBER**

**5e. TASK NUMBER**

**5f. WORK UNIT NUMBER**

**7. PERFORMING ORGANIZATION NAME(S) AND ADDRESS(ES)**

University of Texas at Austin
3925 West Braker Lane
Building 156 (WPR), Suite 3.11072
Austin, TX 78759

**8. PERFORMING ORGANIZATION REPORT NUMBER**

**9. SPONSORING / MONITORING AGENCY NAME(S) AND ADDRESS(ES)**

U.S. Army Medical Research and Materiel Command
Fort Detrick, Maryland 21702-5012

**10. SPONSOR/MONITOR'S ACRONYM(S)**

**11. SPONSOR/MONITOR'S REPORT NUMBER(S)**

**12. DISTRIBUTION / AVAILABILITY STATEMENT**

Approved for Public Release; Distribution Unlimited

**13. SUPPLEMENTARY NOTES**

**14. ABSTRACT**

The overall objective of the proposed research is to develop a set of technologies to enable peripheral neural electrodes that have a high-density contact array, ultra-flexibility, and spatially defined biomaterials that promote neurovascular regeneration. The resulted regenerative neural electrode will be capable of selective interfacing and promote the ingrowth of neural and vascular tissues, which result in a seamless integration of peripheral nerves, vessels and electrode. We proposed the following related specific tasks to create advanced neural interfaces: Task 1. Design and fabrication of high-density ultra-flexible mesh electrodes. Task 2. Create and optimize patternable materials that can specifically induce neurovascular regeneration to stabilize electrode-nerve interaction. Task 3. Construct nerve guidance scaffolds comprising of embedded ultra-flexible mesh electrodes with defined pathways for neurogenesis/angiogenesis and test these scaffolds in a mouse subcutaneous implantation model and a rat sciatic nerve gap model.

**15. SUBJECT TERMS**

None listed.

| 16. SECURITY CLASSIFICATION OF: | | | 17. LIMITATION OF ABSTRACT | 18. NUMBER OF PAGES | 19a. NAME OF RESPONSIBLE PERSON |
|---|---|---|---|---|---|
| a. REPORT | b. ABSTRACT | c. THIS PAGE | | | USAMRMC |
| Unclassified | Unclassified | Unclassified | Unclassified | 20 | 19b. TELEPHONE NUMBER *(include area code)* |

## Table of Contents

**Page**


**1. Introduction……. 3**

**2. Keywords……. 3**

**3. Accomplishments……..……... 3**

**4. Impact……...…… 14**

**5. Changes/Problems...…..…… 15**

**6. Products…….……..…..……. 15**

**7. Participants & Other Collaborating Organizations……. 15**

**8. Special Reporting Requirements…… 17**

**9. Appendices…… 17**

## 1. Introduction

In American there are one out of 190 people that are suffering from limb loss which may due to injury, amputation or neurodegenerative disease [1]. The daily life of those patients is significantly affected by their disability [3]. Advanced neuroprothesis devices bring hope for those patients to regain their impaired motor and sensory functions [4-10]. However, the development of the neuroprothesis devices has long been limited by the performance of the peripheral neural interface [8, 11]. Existing peripheral neural interface do not have: (1) selectivity and high signal to noise interfacing for both recording and stimulation, and (2) long-term stability and high fidelity, both of which are critical for achieving advanced prosthesis with precise control, multiple freedom, and chronic reliability. Therefore, engineering peripheral neural interfaces that afford selectivity, high signal to noise ratio and chronical stability for both recording and stimulation is imperative. In the project, we focus on rationally optimizing neural interfaces using cutting-edge nanoelectronics and regenerative medicine techniques. Upon completion, the expected outcome will lead to enhanced technology to interface peripheral nerves with advanced prosthetic devices and neuroprothesis with unprecedented fidelity and reliability.

## 2. Keywords

Peripheral neural interface, flexible neural electrode, sciatic nerve.

## 3. Accomplishments

**What were the major goals of the project?**

The overall goal of the proposed research is to develop a set of technologies *to create a peripheral neural electrode that has a high-density contact array, ultra-flexibility, and spatially defined biomaterials that promote neurovascular regeneration.* The resulted regenerative neural electrode will be capable of selective interfacing and promote the ingrowth of neural and vascular tissues, which result in a seamless integration of peripheral nerves, vessels and electrode. We proposed the following related specific tasks to create advanced neural interfaces.

**Task 1. Design neural electrodes for high-density and ultra-flexible peripheral neural interface, guided by mathematical modeling.** Their mechanical stiffness will be orders of magnitude smaller than conventional neural electrodes to eliminate their mechanical mismatch with nervous tissue. The volume of the electrodes will be minimized and areal porosity will be maximized to enable neurovascular ingrowth and seamless integration.

**Task 2. Create and optimize patternable materials that can specifically induce neurovascular regeneration to stabilize electrode-nerve interaction**. Two most effective biomaterials will be identified for neurogenesis and angiogenesis. A high-definition patterning method for these materials will be developed based on 3D printing.

**Task 3. Construct nerve guidance scaffolds comprising of embedded mesh electrodes with defined pathways for neurogenesis and angiogenesis and test these scaffolds in subcutaneous implantation models in mice and a sciatic nerve gap model in rats.** Here, we will combine the technologies developed in Task 1 and 2 to develop novel regenerative electrodes. These electrodes will be tested in several animal models to assess regeneration and functionality in neural recording and stimulation.

In the first year of this project, the following work and goals were planned.

| **Task 1.** Design and fabrication of high-density ultra-flexible mesh electrodes. | | |
|---|---|---|
| | Timeline | Finished date |
| **Subtask 1.1.** ***Design and fabrication.*** | Months | |
| Subtask 1.1.1. Optimize stiffness and porosity of the mesh electrode. | 1-3 | 31-Dec-2017 |
| Subtask 1.1.2. Optimized electrode contact material choice. | 3-6 | 31-Mar-2017 |
| Subtask 1.1.3. Optimize mesh electrodes design for rat Sciatic nerve. | 1-6 | 31-Mar-2017 |
| Subtask 1.1.4. Fabricate mesh electrodes design for rat sciatic nerve iteratively. | 6-18 | In progress 50% |
| Milestone(s) Achieved: | | |
| M1. Establish a robust strategy to fabricate mesh electrode. | 6 | 31-Mar-2017 |
| M2. Identify the optimized design and fabricate mesh electrodes for rat sciatic nerve. | 18 | In progress 50% |
| | | |
| **Subtask 1.2.** ***Validation of mesh electrode properties.*** | Months | |
| Subtask 1.2.1. Mechanical property validation. | 3-18 | In progress 70% |
| Subtask 1.2.2. Electrochemical property validation. | 3-18 | In progress 70% |
| Milestone(s) Achieved: | | |
| M3. Identify the optimized design and fabricate mesh electrodes for rat sciatic nerve. | 18 | In progress 70% |

| **Task 2.** Create and optimize patternable materials that can specifically induce neurovascular regeneration to stabilize electrode-nerve interaction. | | |
|---|---|---|
| | **Timeline** | **Finished Date** |
| **Subtask 2.1.** ***High Throughput Assays for Optimizing Scaffold Composition.*** | Months | |
| Subtask 2.1.1. Test of thrombospondin-1. | 1-12 | In progress 70% |
| Subtask 2.1.2. Test of semaphorin-4D. | 1-12 | In progress 70% |
| Subtask 2.1.3. Test of ephrin-A1. | 1-12 | In progress 70% |
| Milestone(s) Achieved: | | |
| M4. Identify optimal neurogenic and angiogenic materials. | 12 | In progress 70% |
| | | |
| **Subtask 2.2.** ***Optimization of 3D Patterning of Neurovascular Scaffolds Using Photomasking and 3D Bioprinting Techniques.*** | Months | |
| Subtask 2.2.1. Develop photo mask patterning methods. | 1-9 | In progress 50% |
| Subtask 2.2.2. Develop 3D printing patterning methods. | 9-18 | 9/1/2017 |
| Milestone(s) Achieved: | | |
| M5. Construct regenerative nanoelectronic neural interface using photopatterning techniques. | 18 | In progress 75% |

**What was accomplished under these goals?**

Our accomplishments over the last year are summarized according to subtasks as follows.

**Subtask 1.1.1.** Optimize stiffness and porosity of the mesh electrode (100% complete).

Mechanical mismatch can lead to unstable interface in short term and can lead to tissue fibrotic reaction in longer term. In order to eliminate the mechanical mismatch between probe and brain tissue, the stiffness of the mesh electrode should be optimized. Here we calculate the deflection force of the probe and explain how probe thickness influence the magnitude of the force.

For shaft-shaped probes, the bending stiffness K:

$$K_s = E_s w h^3/12 \qquad \text{(eq. 1)}$$

$E_s$ is the Young's modulus of the shaft material, $h$ and $w$ are the thickness and the width of the shaft. For better accuracy:

$$K_{NET} = E_{SU8}\left(\frac{h^3 w}{12} - \frac{h_m^3 w_m}{12}\right) + E_m \frac{h_m^3 w_m}{12} \qquad \text{(eq. 2)}$$

$E_{SU8}$ and $E_m$ are the Young's modulus of SU-8 and gold layers respectively ($E_{SU8}$ = 2 GPa, $E_m$ = 79 GPa); $h$ *and* $h_m$ are the thickness of the SU-8 in total and the gold ($h$ = 1 μm, $h_m$= 100 nm); $w$ is the probe width (18 μm) and $w_m$ is the total width of gold interconnects (5 μm). The bending stiffness of a single ribbon can be estimated as $K = 2.0\times10^{-15} N\cdot m^2$. We calculate the deflection force $F = 8eK/l^3$ (eq. 3) to be 2.5 nN which is comparable to single cell traction force, assuming deflection $e$ = 10 μm and probe length $l$ = 400 μm. Combining eq. 2 and eq. 3 we conclude, F is proportional to $h^3$, which means decreasing the thickness of the mesh electrodes is most effective in increasing their flexibility. And when the overall thickness of the probe is approximately 1μm, the force required to deform it is estimated to be in the range of natural forces occur in brain tissues.

In order to promote neural regeneration, we also try to maximize the porosity of the mesh electrode array.

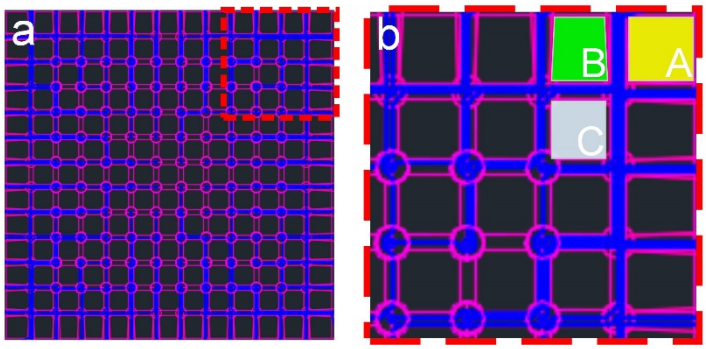


**Figure 1**. the schematic of mesh electrode. (a) The schematic of mesh electrode array. (b) the expanding photo of mesh electrode in (a), A, B, C represent three kind of different pore size.

$$P = \frac{(S_A\times N_A + S_B\times N_B + S_C\times N_C)}{S}$$

The porosity of the designed mesh electrode, P is calculated as follows, $S_A$ $S_B$ $S_C$ are the area of different pores A, B, and C. ($S_A = 7.7\times10^{-3}\ mm^{-3}$ $S_B = 6.6\times10^{-3}\ mm^{-3}$ $S_C = 6.1\times10^{-3}\ mm^{-3}$) $N_A$ $N_B$ $N_C$ are the number of different pores A, B, and C. S is the whole area of the mesh electrode. ($N_A = 4$ $N_B = 44$ $N_C = 121$) The overall porosity of this mesh electrode is 62.7%.

**Subtask 1.1.2.** Optimized electrode contact material choice

We have tested several electrode materials, including gold and platinum, with electrochemical impedance spectroscopy analysis. We concluded that platinum is the more suitable electrode material for the current study because it affords a lower impedance at the electrode-tissue interface, which is expected to provide a higher signal-to-noise ratio.

**Subtask 1.1.3.** Optimize mesh electrodes design for rat Sciatic nerve.

The diameter of neuron axon in rat sciatic nerves ranging from 2 to 10 μm. Therefore, to make it possible for the regenerated axons to grow through, it is necessary to design pores that are at least larger than 10 μm on the mesh electrode. In addition, larger porosity induces less obstacles for the regrowth of nerve fibers. Therefore, in the mesh electrode we designed holes with areas of 80 × 80 μm. And the mesh electrode array covers an overall area of 1.3 × 1.3 mm, which is comparable to the size of the cross-section area of the rat sciatic nerve. A set of 8 photomasks have been designed and manufactured to fabricate the prototype mesh electrode (**Figure 2**).

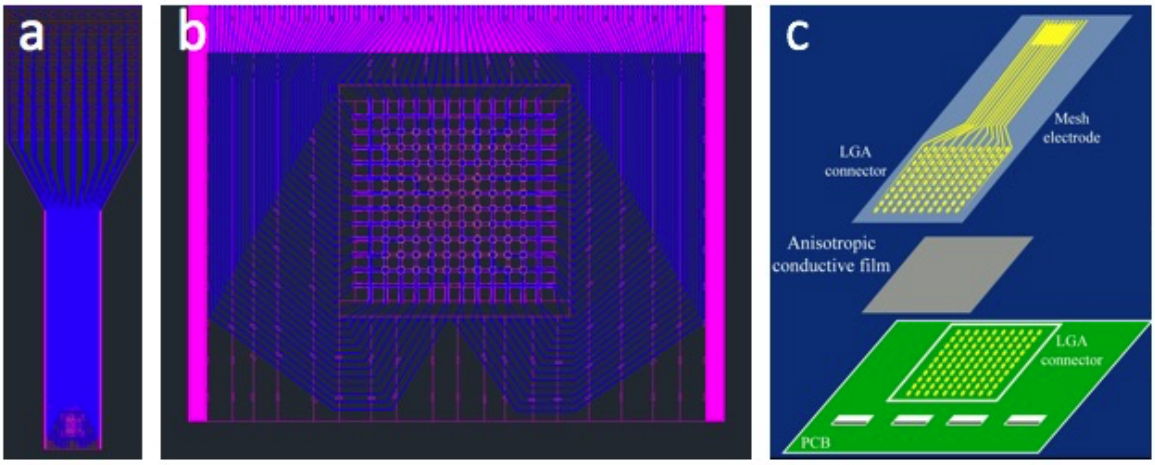


**Figure 2**. Photomask design for the mesh electrode. (a) Overall design. (b) Zoom-in of the electrode array area. (c) Interconnect mechanism.

**Subtask 1.1.4.** Fabricate mesh electrodes design for rat sciatic nerve iteratively.

We have fabricated the first prototype of the mesh electrode. **Figure 3** shows the schematic of the electrode fabrication. The multi-layer probes were fabricated using photolithography on a nickel metal release layer deposited on a silicon substrate (900 nm SiO2, n-type 0.005 V·cm, University Wafer). SU-8 photoresist (SU-8 2000.5, MicroChem Corp.), which offers excellent tensile strength, ease of fabrication and demonstrated durability in ultra-thin structures was used to construct the insulating layers. We used the minimum thickness of the dielectric layer

necessary for preventing more than 1% signal attenuation through the capacitive coupling between the interconnects and the conductive medium surrounding the probe, which was determined to be about 500 nm for our probe geometry and material. Gold and platinum was used for electrodes and interconnects.

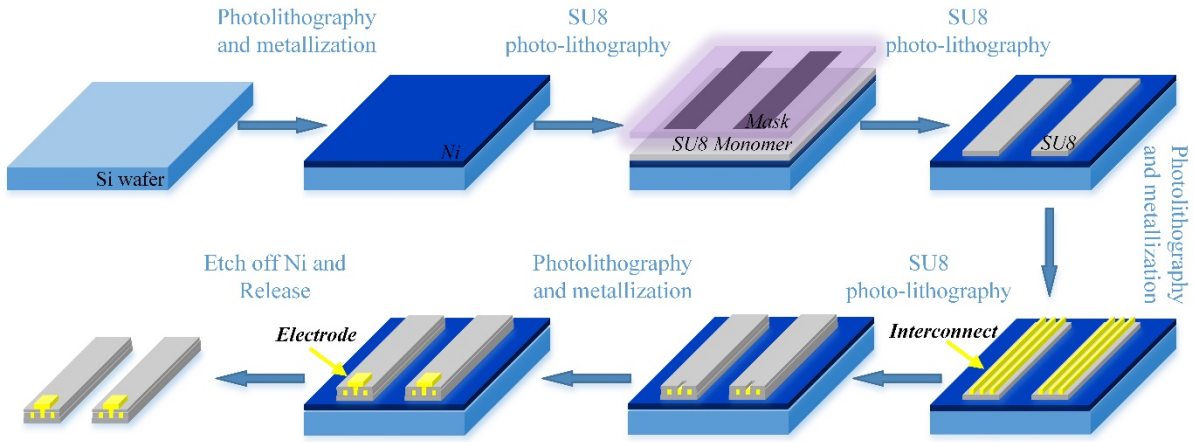


**Figure 3.** schematic of electrode fabrication.

The fabricated mesh electrode shows in **Figure 4**. In **a**, the mesh electrode has three major regions, including the mesh electrode (red square), the interconnection (blue square) and the backend contact array (yellow square). **b, c, d** show the enlarged view of mesh electrode, in which the yellow squares are pores on the mesh electrode, yellow lines covered by transparent red lines are interconnection traces embedded in SU8 isolation layer. **e** shows released electrode in water which represent the ultraflexible property of the mesh electrode.

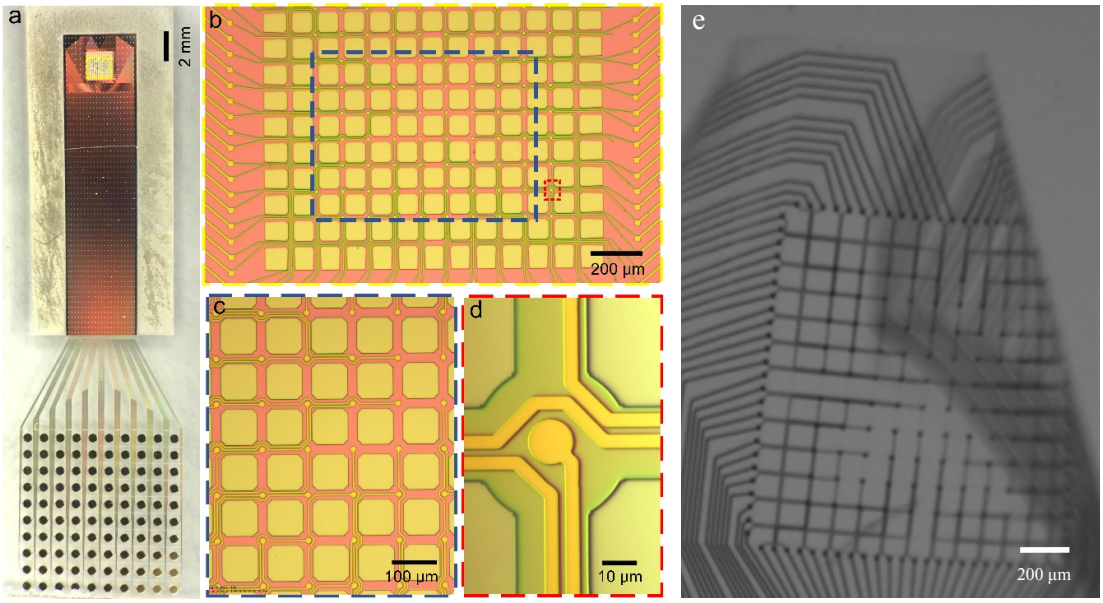


**Figure 4.** The structure of the mesh electrode. (a) Photo of whole electrode. (b) Enlarged view of electrode from (a). (c) Enlarged view from (b). (d) Enlarged view of a single electrode from (b). (e) Mesh electrode released from glass wafer, suspended in water.

**Subtask 1.2.** Validation of mesh electrode properties.
With the first mesh electrode prototype, we started with the evaluation of the electrode's mechanical and electrical properties.

**a)** We measured the porosity of the fabricated mesh electrode using optical microscopy, which confirmed that it is the same as we designed above, 63%.

In comparison with representative published PNS neural electrodes (**Figure 5a**), the estimated bending stiffness and tissue displacement per contact of our prototype mesh electrode are at least four and one orders of magnitude smaller, respectively. We used atomic force microscope measure the bending force of one ribbon of the mesh electrode. (**Figure 5b**) The result proves the bending stiffness of the ribbon are comparable to single cell migration force [12]. These results demonstrated that our first prototype meet the proposed properties of ultraflexibility and ultrasmall tissue displacement.

**b)** We measure the electrode fabrication yield by testing the electrical connection between the contact sites on the mesh electrode and the backend connection pad. The average yield was about 80% for the current prototype. After inspection, we found most yield loss was due to fabrication defects. In the next mesh electrode design, we will implement an optimized design that can minimize defects.

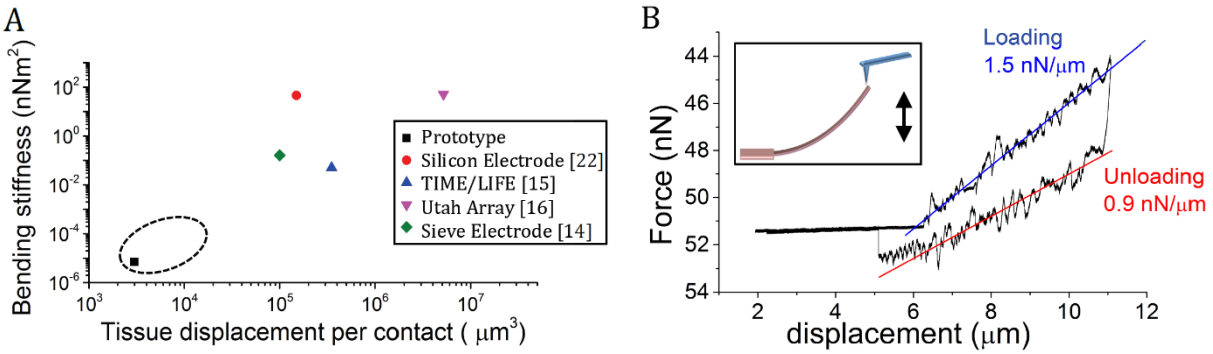


**Figure 5.** Mechanical properties of mesh electrodes. (A) Plot of bending stiffness and tissue displacement per contact for the prototype mesh electrode, in comparison with representative published PNS neural electrodes. The dashed circle indicates the region mesh electrodes can cover. (B) Measurement of the deflection force of mesh grid ribbon by atomic force microscope.

**Progress on Subtask 2.1 High throughput assays for optimizing scaffold composition.**

We tested several candidate polymer systems for use as a regenerative, patternable scaffold material. We first tested the poly(ethylene glycol) diacrylate (PEGDA)-alginate gel blend outlined in the grant proposal. The PEGDA hydrogels polymerized well as seen in **Figure 6**. The prepolymer PEGDA-alginate system was highly viscous which made it difficult to work with in terms of material for patterning by printing technologies. Thus, we were not able to use as high of concentrations as we first anticipated (10% maximum alginate concentration).

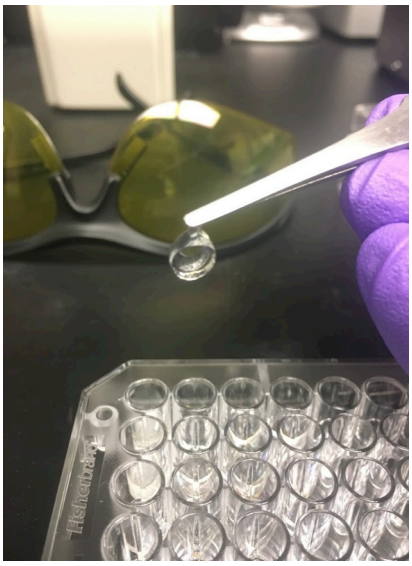

Figure 6. Photoactivated PEGDA hydrogel.

To introduce space into our hydrogel mesh, we hypothesized that the introduction of poly(ethylene glycol) methacrylate (PEGMA) would help increase our mesh size and allow cells to migrate through. We created a combinatorial hydrogel experiment to test the concentrations of PEGDA-PEGMA and PEG linked RGD peptide that would provide the optimal hydrogel mixture to promote cellular migration. We again ran into difficulties with the swelling ratio. The gels when introduced to media, swelled to a high degree, in some cases absorbing 24 times their weight in media. This caused the gels to become displaced in our transwell assay. We consequently decided to examine other materials that would be more amenable to patterning.

The next materials we examined were collagen methacrylate (ColMA) and gelatin methacrylate (GelMA) base materials. These materials had the same photoactivatable properties as the PEGDA gels but also had the distinct benefit of not requiring extra RGD groups to allow cell adhesion. The ColMA was functionalized at ~40% of the lysine residues with a methacrylate group that when exposed to a UV radical photoinitiator would crosslink. When crosslinked, the collagen gels did not experience the same severe swelling phenomenon that the PEGDA gels experienced. We tested collagen gels of varying concentrations in the transwell migration assay that was outlined in our grant proposal. We initially saw some differences in HUVEC and PC12 migration through the gels compared to the collagen coated control (**Figure 7**).

After extensive research into patterning techniques, we found that 10% gelatin methacrylate (GelMA) base gel was the best for performing 3D printing of the gels. Experiments are underway to examine the effect of angiogenesis and neuromodulatory proteins at a range of concentrations between 10 ng/ml of gel to 800 ng/ml of gel.

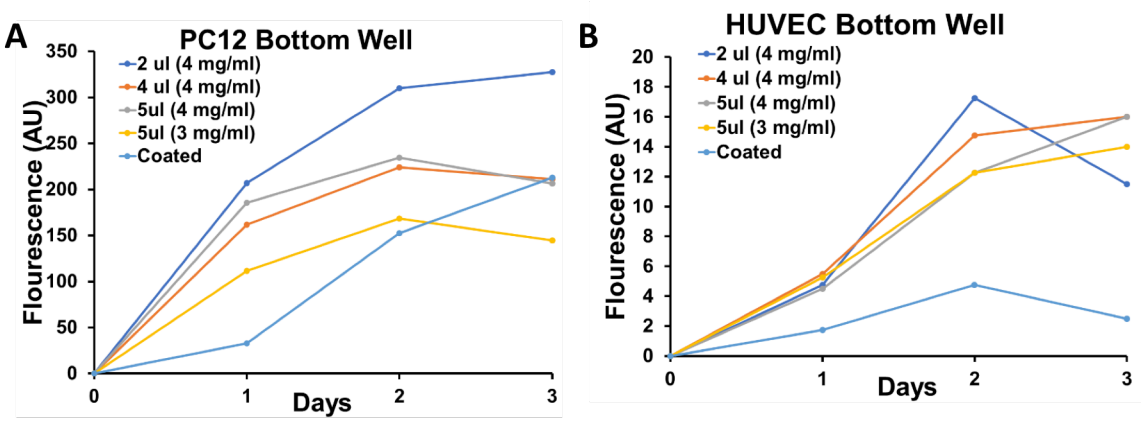


Figure 7. (A) PC12 cellular migration through collagen gels. (B) Migration of endothelial cells through collagen gels.

**Subtask 2.2 Optimization of 3D Patterning of Neurovascular Scaffolds Using Photomasking and 3D Bioprinting Techniques.**

To date, we examined several options in terms of patterning the materials. Our group first tested whether it would be possible to use inkjet printing to print patterns of collagen. This method is highly appealing for its resolution and ability to deliver small volumes of material with high accuracy. We used a Dimatix 2850 printer to deposit 10 pL droplets of collagen (**Figure 8**). However, there was high incidence of occlusion of the print head that hampered the reliability of the method. We experimented with using alterations in pH and detergents but none of the conditions provided materials that would be good for our end application.

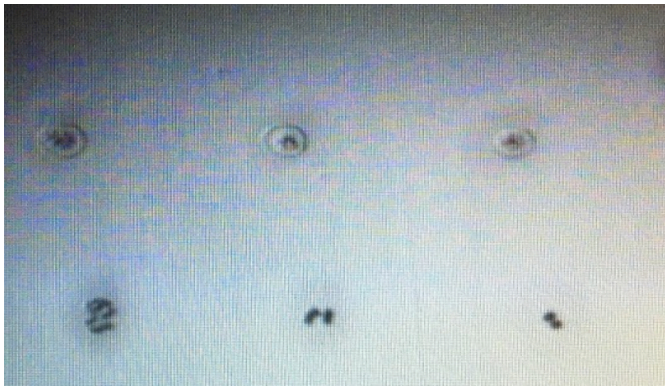

Figure 8. 10 pL droplets of ColMA printed by the Dimatix 2850 inkjet printer.

We next examined using 3D printing technology to achieve patterning. In collaboration with another group, we gained access to the EnvisionTEC Bioplotter to perform the patterning of our gel mixture. We performed an optimization study of the concentration of collagen, print head temperature and stage temperature. The printing method was highly effective and could produce accurate patterns. In **Figure 9**, we

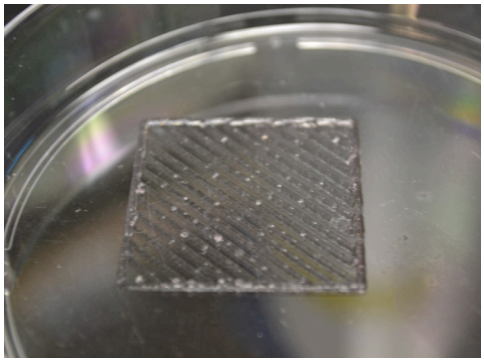

Figure 9. 3D printed gelatin methacrylate produced using the EnvisionTEC Bioplotter.

have patterned gelatin methacrylate at an ~400 um resolution, with a 2 mm offset between the lines. With a smaller needle diameter, we believe we can achieve an even higher resolution. Efforts are currently underway to pattern two materials simultaneously.

**Subtask 3.3. Test regenerative mesh electrodes in a rat sciatic nerve gap model.**

While work on this aim was not in our initial time line, we began studies to validate and establish the model in our laboratory in case there were unexpected difficulties. To this end, we have completed extensive pilot studies in the sciatic nerve gap model. The first goal of the pilot studies was to refine the surgical method. Briefly, the rat is anesthetized and opened at mid-thigh. The muscle is separated along the gap between the biceps femoris and the vastus lateralis and the muscle is pulled back. The sciatic nerve is freed from the surrounding tissue and transected. The devices are placed in the gap and sutured to the epineurium. The muscle is then re-approximated and the wound is stapled closed (**Figure 10**).

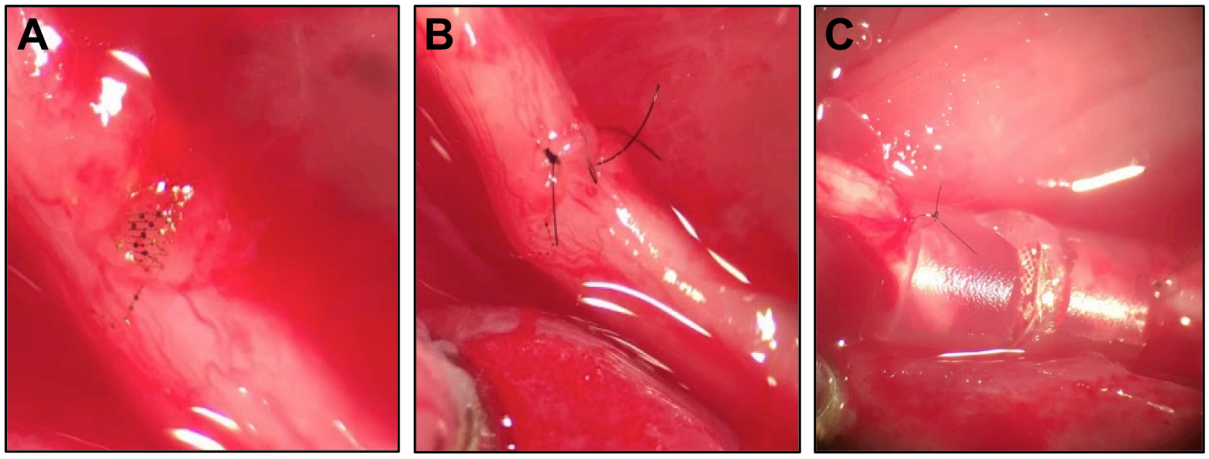


Figure 10. Nerve transection model in the sciatic nerve of rats. (A) Implantation of the unsupported mesh electrode in the sciatic nerve. (B) Suturing of the sciatic nerve. (C) Implantation of the sieve electrode with supporting silicone cuff.

We have completed our pilot studies for the sciatic nerve gap model. The H&E photo shown below shows the mesh electrode that was implanted in a rat sciatic nerve for one month before sacrifice. We have also completed pilot studies for a smaller device for recording and stimulation in the sciatic nerve, shown in **Figure 11**. After completion of the pilot studies we moved on to testing the effects of device thickness.

We have also started the control studies for the sciatic nerve gap model for the regenerative electrode. At the time of this report, a cohort of rats receiving nerve guide implants, and one receiving nerve guides with uncoated regenerative electrodes have been survived for 9 and 8 weeks respectively. These devices are now encased in a nerve guide as shown in **Figure 11A**. We will use force of contraction of the hind limb musculature and conduction velocity through

the sciatic nerve to measure the nerve regeneration and are currently in the process of identifying the system requirements we need to make these measurements.

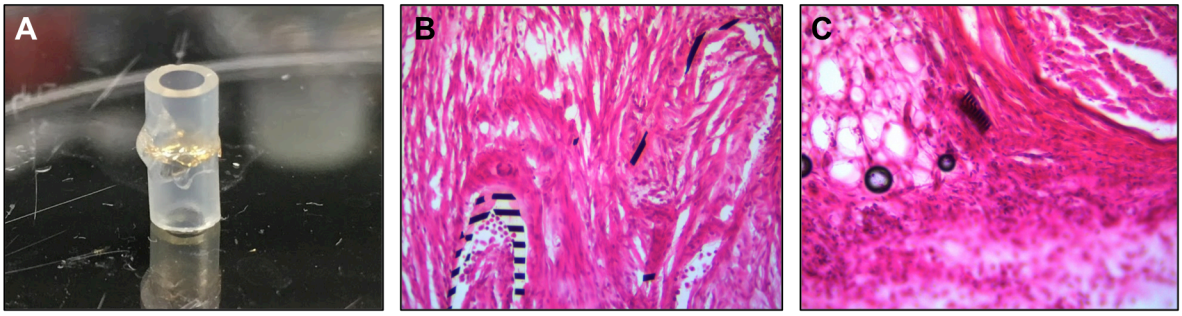

Figure 11. Results of initial studies on with electrode implantation. (A) Sieve electrode with silicone cuff. (B) Histological image of sieve electrode after tissue harvest. (C) Histological image of fiber electrode after implantation.

**What opportunities for training and professional development has the project provided?**
This project has provided the opportunities for graduate students and postdoctoral fellows to conduct their thesis research in a cutting-edge field.

**How were the results disseminated to communities of interest?**
Results have not been disseminated at this time.

**What do you plan to do during the next reporting period to accomplish the goals?**
We plan to finish off the studies to optimize the materials and continue animal testing with the electrodes with patterned materials.

## 4. Impact

**What was the impact on the development of the principal discipline(s) of the project?**
The electrode developed in this project are likely to influence both basic and applied science study, especially the development of neuroprotheses. Nowadays neuro interface in peripheral system can be used for chronically stable stimulation. The limb of prothesis patients can be stimulated to move using machines, however, they still can only use visual as their only feedback which is limited in many ways. So, realizing chronic recording from peripheral systems such as sciatic nerve made it possible to directly get feedback from sensors of human body. In that way people would be able to feel the strength, temperature, pain through their own limbs.

**What was the impact on other disciplines?**
The nanofabrication techniques developed here may be useful in many other fields. In addition, the regenerative technologies that will be developed would be broadly useful in nerve repair and tissue engineering.

**What was the impact on technology transfer?**
None to report.

**What was the impact on society beyond science and technology?**
This work may lead to therapies that can impact the medical care of patients with limb amputation and nerve injury.

## 5. Changes/Problems

None to report.

## 6. Products

Nanoelectronic Coating Enabled Versatile Multifunctional Neural Probes
Z Zhao, L Luan, X Wei, H Zhu, X Li, S Lin, JJ Siegel, RA Chitwood, C Xie
Nano Letters 17 (8), 4588-4595

Ultraflexible nanoelectronic probes form reliable, glial scar–free neural integration
Lan Luan, Xiaoling Wei, Zhengtuo Zhao, Jennifer Siegel, Ojas Potnis, Catherine Tuppen, Shengqing Lin, Shams Kazmi, Robert Fowler, Stewart Holloway, Andrew Dunn, Raymond Chitwood, Chong Xie
Science Advances 3 (2), e1601966

System and method for making and implanting high-density ELECTRODE ARRAYS
US Provisional 62555798

## 7. Participants & other collaborating organizations

| | |
|---|---|
| Name: | Aaron Baker |
| Project Role: | Principal Investigator |
| Researcher Identifier (e.g. ORCID ID): | |
| Nearest person month worked: | 1 |
| Contribution to Project: | Dr. Baker is responsible for the management and leadership of the work in Task 2 and 3. |
| Funding Support: | 1 month |

| | |
|---|---|
| Name: | Chong Xie |
| Project Role: | Principal Investigator |
| Researcher Identifier (e.g. ORCID ID): | |
| Nearest person month worked: | 1 |
| Contribution to Project: | Dr. Xie is responsible for the management and leadership of the work in Task 1 and 3. |
| Funding Support: | 1 month |

| | |
|---|---|
| Name: | Jason Lee |
| Project Role: | Post Doc |
| Researcher Identifier (e.g. ORCID ID): | jl49623 |
| Nearest person month worked: | 10 |
| Contribution to Project: | Dr. Lee has worked on the patterning methods. |
| Funding Support: | Not Applicable |

| | |
|---|---|
| Name: | Austin Veith |
| Project Role: | Graduate Student |
| Researcher Identifier (e.g. ORCID ID): | av29786 |
| Nearest person month worked: | 10 |
| Contribution to Project: | Mr. Veith has worked on the protein screen, developed 3D patterning methods and is the primary surgeon for the animal models. |
| Funding Support: | Not Applicable |

| | |
|---|---|
| Name: | Xue Li |
| Project Role: | Graduate Student |
| Researcher Identifier (e.g. ORCID ID): | |
| Nearest person month worked: | 9 |
| Contribution to Project: | Ms. Li worked on designing, fabricating, testing the performance of the mesh electrode. |
| Funding Support: | 3 months |

| | |
|---|---|
| Name: | Zhengtuo Zhao |
| Project Role: | Graduate Student |
| Researcher Identifier (e.g. ORCID ID): | |
| Nearest person month worked: | 4.5 |
| Contribution to Project: | Ms. Zhao worked on the fabrication of the mesh electrode. |
| Funding Support: | 4.5 months |

| | |
|---|---|
| Name: | Hanlin Zhu |
| Project Role: | Graduate Student |
| Researcher Identifier (e.g. ORCID ID): | |
| Nearest person month worked: | 4.5 |
| Contribution to Project: | Mr. Veith has worked on the protein screen, developed 3D patterning methods and is the primary surgeon for the animal models. |
| Funding Support: | 4.5 months |

## 8. Special Reporting Requirements

None to report.

## 9. Appendices

None to report.

## References


1. Ziegler-Graham, K., MacKenzie, E. J., Ephraim, P. L., Travison, T. G., & Brookmeyer, R. (2008). Estimating the prevalence of limb loss in the United States: 2005 to 2050. *Archives of physical medicine and rehabilitation*, *89*(3), 422-429.

2. Kazmi, S. S., Richards, L. M., Schrandt, C. J., Davis, M. A., & Dunn, A. K. (2015). Expanding applications, accuracy, and interpretation of laser speckle contrast imaging of cerebral blood flow. *Journal of Cerebral Blood Flow & Metabolism*, *35*(7), 1076-1084.

3. Pasquina, P. F., Bryant, P. R., Huang, M. E., Roberts, T. L., Nelson, V. S., & Flood, K. M. (2006). Advances in amputee care. *Archives of physical medicine and rehabilitation*, *87*(3), 34-43.

4. Navarro, X., Krueger, T. B., Lago, N., Micera, S., Stieglitz, T., & Dario, P. (2005). A critical review of interfaces with the peripheral nervous system for the control of neuroprostheses and hybrid bionic systems. *Journal of the Peripheral Nervous System*, *10*(3), 229-258.

5. Erik Scheme MSc, P., & Kevin Englehart PhD, P. (2011). Electromyogram pattern recognition for control of powered upper-limb prostheses: State of the art and challenges for clinical use. *Journal of rehabilitation research and development*, *48*(6), 643.

6. Rothschild, R. M. (2010). Neuroengineering tools/applications for bidirectional interfaces, brain–computer interfaces, and neuroprosthetic implants–a review of recent progress. *Frontiers in neuroengineering*, *3*, 112.

7. Bossi, S., Kammer, S., Doerge, T., Menciassi, A., Hoffmann, K. P., & Micera, S. (2009). An implantable microactuated intrafascicular electrode for peripheral nerves. *IEEE Transactions on Biomedical Engineering*, *56*(11), 2701-2706.

8. Garde, K., Keefer, E., Botterman, B., Galvan, P., & Romero-Ortega, M. I. (2009). Early interfaced neural activity from chronic amputated nerves. *Frontiers in neuroengineering*, *2*, 5.

9. Micera, S., & Navarro, X. (2009). Bidirectional interfaces with the peripheral nervous system. *International review of neurobiology*, *86*, 23-38.

10. Collinger, J. L., Foldes, S., Bruns, T. M., Wodlinger, B., Gaunt, R., & Weber, D. J. (2013). Neuroprosthetic technology for individuals with spinal cord injury. *The journal of spinal cord medicine*, *36*(4), 258-272.

11. Grill, W. M., Norman, S. E., & Bellamkonda, R. V. (2009). Implanted neural interfaces: biochallenges and engineered solutions. *Annual review of biomedical engineering*, *11*, 1-24.

12. Hockaday, L. A., Kang, K. H., Colangelo, N. W., Cheung, P. Y. C., Duan, B., Malone, E., ... & Chu, C. C. (2012). Rapid 3D printing of anatomically accurate and mechanically heterogeneous aortic valve hydrogel scaffolds. *Biofabrication*, *4*(3), 035005.